Eur. Phys. J. A **18**, 527–530 (2003)
DOI 10.1140/epja/i2002-10275-5

**THE EUROPEAN PHYSICAL JOURNAL A**

# Saturation in small-x and heavy-ion physics

A.H. Mueller

Physics Department, Columbia University, New York, NY 10027, USA

Received: 30 September 2002 /
Published online: 22 October 2003 – 

**Abstract.** The idea of parton saturation is reviewed. The use of saturation in describing HERA data is discussed in the context of the McLerran-Venugopalan and Golec-Biernat Wüsthoff models. Applications of saturation ideas to RHIC data are reviewed and a comparison between applications at HERA and at RHIC is given.

**PACS.** 11.10.-z Field theory

## 1 Introduction

*Partons in hadrons and saturation*

The partonic picture of hadrons and the saturation of partons are not easily seen in the same reference frame. We shall choose to describe deeply inelastic lepton-hadron scattering in two distinct frames. One of these frames will make the parton picture manifest while the other will make unitarity limits (saturation) manifest.

### 1.1 The Bjorken frame

In the Bjorken frame one choses the proton momentum to be large and along the $z$-axis while the momentum of the virtual photon is mainly in the transverse direction

$$P_\mu = (p + \frac{m^2}{2p}, 0, 0, p)\,, \tag{1}$$

$$q_\mu = (q_0, q_\perp, 0)\,. \tag{2}$$

As $p \to \infty$, $q_0 = \frac{q\cdot P}{p} \to 0$. The invariants usually chosen to describe the process are $-q_\mu q^\mu = Q^2 \simeq q_\perp^2$ and $x = \frac{Q^2}{2P\cdot q}$ and this latter variable serves to label the momentum fraction, of the original proton momentum $P$, carried by the struck quark. The process is illustrated in fig. 1.

The virtual photon is absorbed over a length scale $\Delta x_\perp \simeq 1/q_\perp = 1/Q$ and during a time $\Delta t = (E_k + E_q - E_{k+q})^{-1} \simeq 1/Q$. The time of absorption and the region of absorption in the proton are so small, for large $Q$, that the absorption must take place on single quarks or antiquarks in the wave function of the proton. This makes the following formula natural:

$$F_2(x, Q^2) = \sum_f e_f^2 [x q_f(x, Q^2) + x\bar{q}_f(x, Q^2)]\,, \tag{3}$$

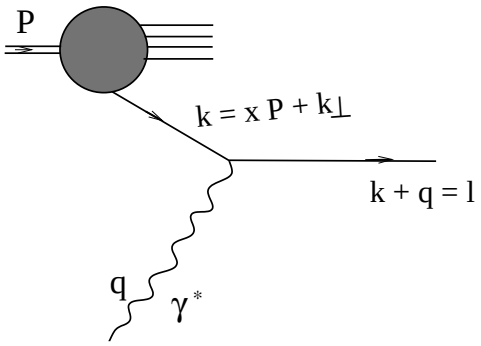


**Fig. 1.**

where $q_f$ and $\bar{q}_f$ are the quark and antiquark number densities in the proton, and $e_f$ is the quark charge as a fraction of the charge of the proton.

### 1.2 The dipole frame

The Bjorken frame shows deep inelastic scattering in terms of the quark components of the infinite-momentum wave function of the proton. There is an alternate view where one still gives the proton a large momentum but where now the $\gamma^*$ also has a sufficiently large longitudinal momentum so that the process can be viewed as $\gamma^* \to q\bar{q}$ and then the $q\bar{q}$ dipole scatters on a highly developed wave function of the proton as illustrated in fig. 2. The momenta can be given as

$$P = (p + \frac{m^2}{2p}, 0, 0, p)\,, \tag{4}$$

$$q = (\sqrt{q^2 - Q^2}, 0, 0, q)\,, \tag{5}$$

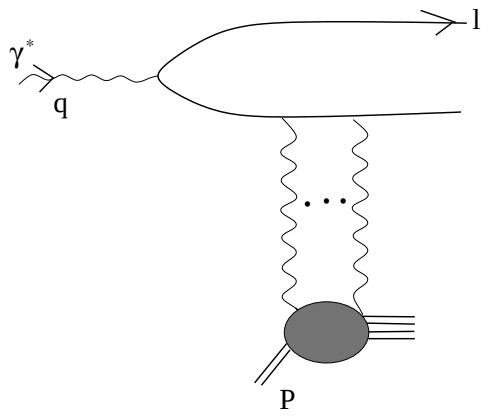


**Fig. 2.**

where $q/Q > 1$ but not too large. QCD evolution is still in the proton. We shall see below that parton scattering corresponds to the unitarity limit of dipole scattering on the proton.

## 2 Simple models of saturation in nuclei

It is simplest to illustrate saturation in deep inelastic scattering by using a large nucleus to create large quark and gluon number densities. Most of what occurs in a large nucleus can be taken over to protons where it is BFKL evolution which there creates large parton densities.

### 2.1 Quark saturation

We are going to calculate $\frac{\mathrm{d}x(q+\bar{q})}{\mathrm{d}^2b\mathrm{d}^2\ell_\perp}$, the sea quark distribution of light quarks per unit of transverse phase space in the nuclear wave function [1]. One can view the cross-section for producing a quark jet either as in fig. 1, where the partonic interpretation is clear, or as in fig. 2, where the scattering of the dipole on a large nucleus can be done in the multiple scattering approximation. In this latter picture one easily finds [1]

$$\begin{aligned}\frac{\mathrm{d}x(q_f+\bar{q}_f)}{\mathrm{d}^2b\mathrm{d}^2\ell_\perp} = &\int \mathrm{d}^2x_1\mathrm{d}^2x_2 e^{-i\ell_\perp\cdot(x_{1\perp}-x_{2\perp})}\\ &\times\int_0^1\mathrm{d}z\Big\{\frac{Q^2N_c}{32\pi^6}\,[z^2+(1-z^2)]\\ &\times\nabla_{x_1}K_0\Big(\sqrt{Q^2x_{1\perp}^2z(1-z)}\,\Big)\\ &\times\nabla_{x_2}K_0\Big(\sqrt{Q^2x_{2\perp}^2z(1-z)}\,\Big)\Big\}\\ &\times\Big[1+e^{-(x_{1\perp}-x_{2\perp})^2\bar{Q}_s^2/4}-e^{-x_{1\perp}^2\bar{Q}_s^2/4}\\ &-e^{-x_{2\perp}^2\bar{Q}_s^2/4}\Big],\end{aligned}\tag{6}$$

where

$$\bar{Q}_s^2=\frac{C_F}{C_A}\,Q_s^2=4/9Q_s^2\tag{7}$$

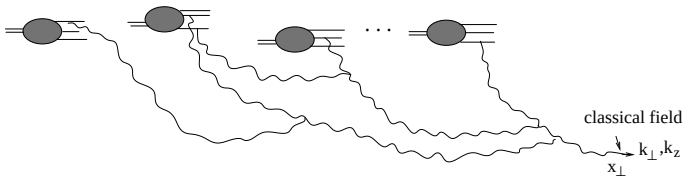


**Fig. 3.**

and

$$Q_s^2=\frac{4\pi^2\alpha N_c}{N_c^2-1}\,2\sqrt{R^2-b^2}\;\rho xG.\tag{8}$$

In (6) $x_{1\perp}$ is the transverse coordinate of the measured quark in the amplitude and $x_{2\perp}$ is the corresponding coordinate in the complex conjugate amplitude. The term $\{\}$ in (6) is $\frac{1}{8\pi^2}\psi_\gamma^*(x_{2\perp})\psi_\gamma(x_{1\perp})$; $\rho$ is the nuclear density; $xG$ is the gluon density of a nucleon, and $b$ is the impact parameter of the nucleus. The four terms in [ ] in (6) correspond to no interactions, an arbitrary number of interactions in the amplitude and in the complex conjugate amplitude, an arbitrary number of interactions in the amplitude with no interactions in the complex conjugate amplitude, and an arbitrary number of interactions in the complex conjugate amplitude with none in the amplitude, respectively. Thus, for example, the third term

$$S(x_{1\perp},b)=\bar{e}^{x_{1\perp}^2Q_s^2(b)/4}\tag{9}$$

is the $S$-matrix for the interaction of a dipole of size $x_{1\perp}$ with the nucleus at impact parameter $b$. Unitarity is imposed by the fact that $|S|\le 1$ and $S\to 0$ for large $x_{1\perp}^2$.

Saturation show up when $\ell_\perp^2/Q_s^2\ll 1$ in which case (6) gives [1]

$$\frac{\mathrm{d}^2x(q_f+\bar{q}_f)}{\mathrm{d}^2b\mathrm{d}^2\ell_\perp}=\frac{N_c}{2\pi^4}\tag{10}$$

a remarkable result which says that the number of quarks in the nucleus cannot grow too big in a given region of phase space. This can be turned (approximately) into a 3-dimensional occupation number:

$$f_q=\frac{(2\pi)^3}{2\cdot 2\cdot N_c}\,\frac{\mathrm{d}x(q_f+\bar{q}_f)}{\mathrm{d}^2b\mathrm{d}^2\ell_\perp}=\frac{1}{\pi}\,,\tag{11}$$

where the two factors of 2 in the denominator count particle and antiparticle and spin factors.

### 2.2 Gluon saturation (McLerran-Venugopalan model) [2]

Quark saturation occurs at the one fermionic loop level and is purely a quantum phenomenon. Gluon saturation, on the other hand, occurs at the semiclassical level and for a large nucleus corresponds to graphs like those shown in fig. 3 in the Bjorken frame and in a particular light-cone gauge [3]. One finds [4,5]

$$\frac{\mathrm{d}xG}{\mathrm{d}^2b\mathrm{d}^2\ell_\perp}=\frac{N_c^2-1}{4\pi^4\alpha N_c}\int\frac{\mathrm{d}^2x_\perp}{x_\perp^2}e^{-i\ell_\perp\cdot x_\perp}\Big(1-e^{-x_\perp^2Q_s^2/4}\Big).\tag{12}$$

When $\ell_\perp^2/Q_s^2 \gg 1$ the additive result is recovered while for $\ell_\perp^2/Q_s^2 \ll 1$

$$\frac{\mathrm{d}xG}{\mathrm{d}^2b\mathrm{d}^2\ell_\perp} = \frac{N_c^2-1}{4\pi^3}\ln(Q_s^2/\ell_\perp^2) \tag{13}$$

or

$$f_g = \frac{(2\pi)^3}{2(N_c^2-1)}\,\frac{\mathrm{d}^2xG}{\mathrm{d}^2b\mathrm{d}^2\ell_\perp} = \frac{1}{\alpha N_c}\ln(Q_s^2/\ell_\perp^2). \tag{14}$$

Now occupation numbers are of order $1/\alpha$ which signals a strongly nonlinear classical field theory. Higher orders will likely modify the constants in (13), but the general form, including $\ln Q_s^2/\ell_\perp^2$, are expected to be general [1,6–8].

## 3 Application to HERA phenomenology

Refer back to (6) which can be written as

$$\begin{aligned}\frac{\mathrm{d}x(q_f+\bar{q}_f)}{\mathrm{d}^2b\mathrm{d}^2\ell_\perp} &= \frac{1}{8\pi^2}\int \mathrm{d}^2x,\mathrm{d}^2x_2\int_0^1 \mathrm{d}z e^{-i\underline{\ell}\cdot(\underline{x}_1-\underline{x}_2)}\\ &\times\psi_\gamma^*(x_{1\perp},z,Q)\psi_\gamma(x_2,z,Q)\\ &\times\Big[1+e^{-(x_{1\perp}-x_{2\perp})^2\bar{Q}_s^2/4}-e^{-x_{1\perp}^2\bar{Q}_s^2/4}-e^{-x_{2\perp}^2\bar{Q}_s^2/4}\Big],\end{aligned} \tag{15}$$

again for a large nucleus. If we integrate over $\mathrm{d}^2\ell_\perp$ and $\mathrm{d}^2b$ with the replacement $\mathrm{d}^2b \to \sigma_0$ on the right-hand side of (15), one obtains

$$\begin{aligned}F_2(x,Q^2) &= \sigma_0\int\sum_f e_f^2\mathrm{d}^2x_\perp\\ &\times\int_0^1 \mathrm{d}z|\psi_\gamma(x_\perp,z,Q)|^2\Big(1-e^{-x_\perp^2Q_s^2/4}\Big).\end{aligned} \tag{16}$$

Taking this form for a proton gives the Golec-Biernal–Wüsthoff model [9]. For diffractive scattering

$$\begin{aligned}F_2^D &= \sigma_0\int\sum_f e_f^2\mathrm{d}^2x_\perp\int_0^1\mathrm{d}z|\psi_\gamma|^2\\ &\times\frac{1}{2}\Big(1-e^{-x_\perp^2Q_s^2/4}\Big)^2 + q\bar{q}g \text{ state.}\end{aligned} \tag{17}$$

The Golec-Biernat–Wüsthoff model has just three parameters

$$\sigma_0 = 23\,\mathrm{mb},\quad \bar{Q}_s^2 = (\frac{x_0}{x})^{0.3}\,\mathrm{GeV}^2,\quad x_0 = 3\times10^{-4}. \tag{18}$$

In general the exponential form for the $S$-matrix as given in (9) cannot be expected to work for protons in detail. However, the general characteristics $S \underset{x_\perp\to 0}{\longrightarrow} 1$ and $S \underset{x_\perp\to\text{large}}{\longrightarrow} 0$ as well as the fact that the corrections to $1-S$ are of order $x_\perp^2$ at small $x_\perp$ are general results which are nicely built into the Golec-Biernat–Wüsthoff model.

The Golec-Biernal–Wüsthoff model works surprisingly for fits to $F_2$ and $F_2^D$ at HERA. There are also now many variations on the model [10–12] which try to reflect more precisely QCD constraints.

## 4 Application to heavy-ion phenomenology

Once densities of produced quarks and gluons in heavy-ion collisions are large enough to be in the quark-gluon phase it does not make sense to try and describe the collision in terms of hadrons. On the other hand, QCD perturbation theory may not give reliable numerical results, but it should be a reasonably accurate guide to the production and early stages of a heavy-ion collision.

### 4.1 The production of gluons

In a head-on heavy-ion collision production in the central rapidity region should be dominated by gluons [13]. It is convenient to view the collision as a right-moving collection of gluons, the wave function of the right-moving nucleus, colliding with a stationary nucleus. Then the primary effect of the collision is to free all the right-moving gluons whose transvese momentum is below the saturation momentum [13].

To try and get some reasonable estimates, we use the McLerran-Venugopalan model as a model for the gluons in the right-moving nucleus. This gives the gluons in the wave function according to (12) above. Just after the collision we suppose that a good fraction of the gluons having $\ell_\perp/Q_s < 1$ have been liberated. Thus we write for the initial gluon distribution produced in the collision

$$\frac{\mathrm{d}N_g}{\mathrm{d}^2b\mathrm{d}\eta} = c\frac{N_c^2-1}{4\pi^2\alpha N_c}Q_s^2\,, \tag{19}$$

where $c$ accounts for the fact that not all gluons may be freed in the collision.

Krasnitz and Venugopalan [14] and Krasnitz, Nara and Venugopalan [15] calculate $\frac{\mathrm{d}N_g}{\mathrm{d}^2b\mathrm{d}\eta}$ numerically using classical Yang-Mills field equations starting from McLerran-Venugopalan wave functions for the colliding nuclei. They find

$$\frac{\mathrm{d}N_g}{\mathrm{d}^2b\mathrm{d}\eta} = \frac{1}{g^2}f_N\Lambda_s^2\,, \tag{20}$$

where $\frac{1}{4\pi}\Lambda_s^2\ln Q_s^2/\Lambda_{\mathrm{QCD}}^2 = Q_s^2$. One gets [16]

$$c = \frac{4\pi^2 f_N}{(N_c^2-1)\ln Q_s^2/\Lambda_{\mathrm{QCD}}^2} \simeq \frac{1}{2} \tag{21}$$

for the calculated value, $f_N \simeq 0.3$.

### 4.2 The production of charged hadrons

Now take (19), integrate over $\mathrm{d}^2b$ and include a factor of $R$ to account for gluon inelasticity as the gluon system evolves toward equilibrium and also include a factor of 2/3 to account for the fraction of produced particles, mostly pions, which are charged. One gets

$$\frac{\mathrm{d}N_{\mathrm{ch}}}{\mathrm{d}\eta} = \frac{2}{3}Rc\frac{N_c^2-1}{4\pi^2\alpha N_c}\int \mathrm{d}^2bQ_s^2. \tag{22}$$

Using (8) along with $xG \simeq \frac{1}{2}\ln Q_s^2/\Lambda_{\rm QCD}^2$, one finds [17]

$$\frac{2}{N_{\rm part}}\frac{{\rm d}N_{\rm ch}}{{\rm d}\eta} = \frac{Rc}{3}\ln Q_s^2/\Lambda_{\rm QCD}^2\,, \tag{23}$$

where the number of participants in the reaction is

$$N_{\rm part} = 2A = 2\int {\rm d}^2b\rho 2\sqrt{R^2-b^2}. \tag{24}$$

We shall now use (23) to help summarize various, closely related, approaches to charged-particle production at RHIC.

#### 4.2.1 Kharzeev, Nardi and Kharzeev, Levin, Nardi picture [17–19]

Here one supposes $R = 1$. Using the experimental value $\frac{2}{N_{\rm part}}\frac{{\rm d}N_{\rm ch}}{{\rm d}\eta} \simeq 3.8$ at $\sqrt{s} = 200$, one sees from (23) that one needs $c \simeq 2.5-3$ for $Q_s^2 = 1-2\,{\rm GeV}^2$. The centrality dependence and energy dependence come out well in this model as well as the $\eta$-dependence.

#### 4.2.2 Krasnitz, Nara, Venugopalan model [14,15]

This model is close to that of Kharzeev *et al.* The authors take McLerran-Venugopalan initial conditions and solve classical Yang-Mills equations to determine the number of gluons radiated during an ion-ion collision. They determine as initial conditions for the freed gluons

$$\frac{{\rm d}N_g}{{\rm d}^2b{\rm d}\eta} = \frac{1}{g^2}f_N\Lambda_s^2 \quad \text{with} \quad f_N \simeq 0.3 \tag{25}$$

and

$$\langle E_T^g\rangle \simeq \frac{3}{2}\Lambda_s. \tag{26}$$

One gets (23) for $\Lambda_s \simeq 1.1-1.3\,{\rm GeV}$ and with $R \simeq 2$–$2.5$.

#### 4.2.3 "Bottom-up" picture [16]

The "bottom-up" picture uses the Boltzman equation, and especially the inelastic collision term in the Boltzmnn equation, to follow the initially freed gluons, coming from a McLerran-Venugopalan distribution, to the time of equilibration. In this picture (23) also emerges. If $c \simeq 1$ and $R \simeq 3$, one finds that equilibration occurs at a time $\simeq 3.5$ fm and at a temperature $T_{\rm eq} \simeq 230\,{\rm MeV}$.

### 4.3 Problems with the models

Although saturation models give results which are generally compatible with the early RHIC results there are a few difficulties which particular versions of the model have.

i) Kharzeev *et al.* need a value of $c$ which is much larger than the value obtained from numerical calculation.

ii) In order to fit the RHIC data Krasnitz, Nara and Venugopalan take $\Lambda_s^2 \simeq 1$–$1.5\ {\rm GeV}^2$, while the McLerran-Venugopalan model gives

$$\Lambda_s^2 \simeq \frac{1}{2}\,{\rm GeV}^2\,.$$

iii) Baier *et al.* need $c \simeq 1$, while the calculations give $c \leq 1/2$. Also analytic calculations are dangerous when $Q_s^2$ is as small as $1\,{\rm GeV}^2$.

iv) The Golec-Biernat–Wüsthoff model gives

$$Q_s^2 = \left(\frac{3x10^{-4}}{x}\right)^{0.3}\cdot\frac{N_c}{C_F} \tag{27}$$

for protons. At $x = 10^{-2}$ this gives $Q_s^2 \simeq 0.8\,{\rm GeV}^2$, while the McLerran-Venugopalan model gives about the same value for gold at $x = 10^{-2}$. The values of $Q_s^2$ do not match too well between RHIC and HERA.

This work has been supported in part by the Department of Energy, Columbia University, New York.

## References


1. A.H. Mueller, Nucl. Phys. B **558**, 285 (1999).
2. L. McLerran, R. Venugopalan, Phys. Rev. D **49**, 2233; 3352 (1994); **50**, 2225 (1994).
3. Yu.V. Kovchegov, Phys. Rev. D **54**, 5463 (1996); **55**, 5445 (1997).
4. J. Jalilian-Marian, A. Kovner, L. McLerran, H. Weigert, Phys. Rev. D **55**, 5414 (1997).
5. Yu.V. Kovchegov, A.H. Mueller, Nucl. Phys. B **529**, 451 (1998).
6. E. Iancu, A. Leonidov, L. McLerran, hep-ph/0202270.
7. E. Iancu, A. Leonidov, L. McLerran, Nucl. Phys. A **692**, 583 (2001).
8. E. Ferreiro, E. Iancu, A. Leonidov, L. McLerran, Nucl. Phys. A **703**, 489 (2002), hep-ph/0109115.
9. K. Golec-Biernat, M. Wüsthoff, Phys. Rev. D **59**, 014017 (1999); **60**, 114023 (1999).
10. J. Bartels, R. Golec-Biernat, H. Kowalski, Phys. Rev. D. **66**, 014001 (2002), hep-ph/0203258.
11. J.R. Forshaw, G. Kerley, G. Shaw, Phys. Rev. D **60**, 074012 (1999); Nucl. Phys. A **675**, 80 (2000).
12. M. McDermott, L. Frankfurt, V. Guzey, M. Strikman, Eur. Phys. J. C **16**, 641 (2000).
13. J.-P. Blaizot, A.H. Mueller, Nucl. Phys. **289**, 747 (1987).
14. A. Krasnitz, R. Venugopalan, Nucl. Phys. B **557**, 537 (1999); Phys. Rev. Lett. **86**, 1717 (2001).
15. A. Krasnitz, Y. Nara, R. Venugopalan, Phys. Rev. Lett. **87**, 192302 (2001).
16. R. Baier, A.H. Mueller, D. Schiff, D.T. Son, Phys. Lett. B **502**, 51 (2001); **539**, 46 (2002), hep-ph/0204211.
17. D. Kharzeev, M. Nardi, Phys. Lett. B **507**, 121 (2001).
18. D. Kharzeev, E. Levin, Phys. Lett. B **523**, 79 (2001).
19. D. Kharzeev, E. Levin, M. Nardi, hep-ph/0111315.